ADSORPTION AND AGEING OF WATER VAPOUR IN ACTIVATED CARBONS

Krisztina László, Department of Physical Chemistry and Materials Science, Budapest University of Technology and Economics, H-1521 Budapest, Hungary
Erik Geissler, Laboratoire de Spectrométrie Physique CNRS UMR 5588, Université J. Fourier de Grenoble, BP 87, 38402 St Martin d'Hères cedex, France

Introduction

Water molecules are of particular importance in activated carbon-vapour phase interactions, since under real conditions, due to relative humidity, they often compete for adsorption sites with other target molecules. In this competition, duration and conditions of storage prior to use could be crucial factors. Little is known, however, about the time scale over which water vapour establishes equilibrium in activated carbons.

Small angle X-ray scattering (SAXS) furnishes structural information on adsorbent-adsorbate systems in the nanometre scale range. Since molecules adsorbed inside the pores modify the electronic contrast of their immediate surroundings, the SAXS signal of the local carbon matrix is sensitive to the adsorbed layer. By comparing the modified signal with that of the dry sample, structural information can be deduced about the adsorbed phase (Hoinkis, Mitropoulos et al, Ramsay, Antxustegi et al, Lozano-Castello). The contrast variation associated with this phenomenon allows the pore filling process to be monitored. However, incomplete wetting by the polar molecules can give rise to cluster formation, which is strongly influenced by hetero-atoms decorating the carbon surface. Cluster formation complicates the analysis of the SAXS signal, since it generates a ternary system composed of the carbon substrate, the condensed liquid phase and the vapour phase.

This paper is based on complementary adsorption and X-ray scattering techniques. The filled status of the pores calculated from adsorption/desorption isotherms depends on the specific adsorption model employed, while small angle X-ray scattering (SAXS) furnishes direct information on the spatial occupation. SAXS observations are reported on amorphous carbons of different origin after equilibration with water vapour at various degrees of relative humidity. Selected samples were first exposed to water vapour then sealed and subsequently aged for different periods of time prior to the measurements. Activated carbons of different surface chemistry were used. Pore filling by water is found to depend on contact time, ageing time and surface composition of the carbon.

Experimental

Two types of activated carbons were investigated, the first prepared from carbonised poly(ethylene terephthalate) (PET), and the second a commercial carbon, R1, kindly supplied by Norit. For the former, the samples were chemically modified to varying degrees by oxidation with nitric acid (Bóta et al). The steam-activated carbon, obtained at 900 °C, was treated for 3 hours with concentrated nitric acid at room temperature (APETA) and at the boiling point of the carbon – acid suspension (APETB) to achieve different degrees of surface functionalization. These acidic samples were washed with distilled water and extracted in a Soxhlet apparatus until neutral pH was attained. The surface chemistry and morphology of these carbons have been characterized elsewhere (László et al. 2005, László et al. 2004)]. The Norit R1 samples were used as received.

Nitrogen adsorption/desorption isotherms, measured at 77 K with a Quantachrome Autosorb-1 instrument, were of Type I, as also discussed previously (László et al. 2004). The surface areas obtained from the BET and the Dubinin-Radushkevich (DR) models for APETA were 1114 and 1293 m^2/g, respectively. For APETB, however, the hot nitric acid treatment reduced the surface area to less than 340 m^2/g, but the pore size distribution in the micropore range nevertheless remained practically unaffected. Average pore widths, derived from the ratio of the total pore volume to the surface area assuming slit shaped geometry, were respectively 8.6 and 9.2 Å for APETA and APETB. The true densities d_{He} of the same samples, determined by helium pycnometry with the same AUTOSORB-1 instrument, were 1.82 and 1.50 g/cm^3. Water vapour adsorption isotherms were measured on a volumetric Hydrosorb apparatus (Quantachrome) at 20°C. The equilibration pressure did not change by more than 0.05 mmHg over a period of 60 s. Data points were recorded after 2000 s whether or not the pressure had equilibrated, unless the pressure fell too far from target pressure (<0.05 % of P_0).

SAXS measurements on the BM2 beam line at the European Synchrotron Radiation Facility (ESRF), Grenoble, France were made at two different wavelengths, λ_0=1.57 Å and 0.69 Å, in the wavevector range 0.008 $Å^{-1} \leq q \leq 5$ $Å^{-1}$. An indirect illumination CCD detector (Princeton Instruments) with 50 µm effective pixel size was used. Intensity curves $I(q)$, obtained by azimuthal averaging, were corrected for grid distortion, dark current, sample transmission and variations of the incident beam intensity, as well as for background scattering.

The samples were powdered in a ball mill to about 0.3 mm particle size, then inserted into 1.5 mm diameter Lindemann glass capillaries and heated to 110°C for 24 hours to remove trapped or adsorbed water. The capillaries were equilibrated in air containing water vapour at 11-98% relative humidity (RH) for 4 weeks and then sealed. This equilibration time is much longer than that employed to measure a complete gas adsorption cycle (ca. 1 day). The SAXS measurements were made at the same temperature as the sample preparation (20°C).

Theoretical Background

The intensity of X-rays of wavelength λ scattered through an angle θ by a carbon sample in dry air is governed both by the structure factor of the carbon, $S_1(q)$, and the difference in electron density ρ_C between the carbon and air. Thus,

$$I_1(q)=r_0^2\rho_C^2\,S_1(q) \tag{1}$$

In Eq. (1), r_0 is the classical radius of the electron and q is the magnitude of the transfer wave vector for X-rays, $q=(4\pi/\lambda)\sin(\theta/2)$. The electron density of the carbon is

$$\rho_C=Zd_{He}N_A/M \tag{2}$$

where Z is the atomic number, M the atomic mass, d_{He} the helium density of the sample and N_A Avogadro's number. If the sample is impregnated with a fluid that only partly fills the unoccupied space in the carbon, the expression for the scattered intensity becomes that of a ternary system, namely

$$I_{tern}(q) = r_0^2\{(\rho_C-\rho_l)^2\,S_{cl}(q)+ \rho_C^2\,S_{cv}(q)+ 2\rho_C(\rho_C-\rho_l)S_{lv}(q)\} \tag{3}$$

where ρ_l is the electron density of the condensed liquid, $S_{cl}(q)$ is the partial structure factor describing the relative positions of carbon and liquid, $S_{cv}(q)$ that between carbon and vapour phase, while $S_{lv}(q)$ is that between liquid and vapour phase. Far from critical conditions, the electron density of the vapour phase is negligible compared to that of the liquid and is equivalent to a vacuum. Owing to the dispersed nature of micropores in carbons, however, in many cases the effective liquid-vapour interface is very small and regions in the carbon in which the fluid is condensed are physically separated from those in which only the vapour phase is present. In such a case the last term in Eq. (3) is negligible and the first two terms can be represented by a pseudo-binary expression

$$I_2(q)= r_0^2\,(\rho_C-\rho_S)^2\,S_2(q). \tag{4}$$

where $(\rho_C-\rho_S)^2S_2(q)$ is an average over the regions in the sample where the fluid is condensed and where it is not. Since these two regions generally have different characteristic sizes and therefore contribute to different zones in q-space, it is reasonable to attribute a q-dependence to ρ_S, i.e., $\rho_S(q)=p(q)\rho_l$, where ρ_l is the density of the condensed fluid and $p(q)$ is the relative density of the fluid with respect to its bulk value. Provided the fluid does not alter the structure of the carbon, $S_1(q)$ and $S_2(q)$ both describe the same total structure factor of the carbon and hence $S_1(q) = S_2(q)$. If the pores are uniformly filled then the two signals $I_1(q)$ and $I_2(q)$ are everywhere proportional to each other, i.e., ρ_S and $p(q)$ are independent of q. If, however, the fluid is not uniformly distributed, e.g., molecules condense only in the finest pores while remaining in the vapour state elsewhere, then the deviations from uniform filling may be expressed by the intensity ratio

$$u(q)= I_2(q)/I_1(q)= [\rho_C-p(q)\rho_l]^2/\rho_C^2, \tag{5}$$

Hence

$$p(q)= \rho_C\,[1- u(q)^{1/2}]\,/\rho_S \tag{6}$$

In principle, $0 \le p(q) <1$ when the pores are incompletely filled. Strongly negative values of $p(q)$ can occur, however, if extended regions of contact exist between the condensed liquid phase and its vapour. This extra scattering, corresponding to the third term in Eq. (3), which is neglected in the pseudo-binary model of independent scattering regions, indicates cluster formation in the sample. In this case, to determine the partial structure factors of Eq. (3), full contrast variation techniques are required, e.g., by solvent deuteration combined with small angle neutron scattering. However, since perturbations from the ternary component tend to be confined to low values of q, the binary model can retain its validity at large q.

Results and Discussion

The nitrogen adsorption isotherms at 77K of all the samples are of Type I, while with water vapour APETA and R1 display isotherms of Type V, owing to the weak interaction between the graphene layers and the water, as a result of the small number of polar sites. The hot nitric acid treatment results in a threefold increase in the surface oxygen concentration, which transforms the water vapour isotherm of APETB from concave to convex shape: the introduced oxygen functionalities increase the affinity for water of the carbon surface.

Figure 1 exemplifies the SAXS spectrum of a dry sample (APETA). In region (*a*) at low q, the spectrum is dominated by surface scattering from grain boundaries within the powder particles. The size of the constituent grains is approximately 1μm (László et al. 2004) and the power-law behaviour visible here, $I(q)\propto q^{-4}$, is due to scattering

from smooth interfaces (Porod). In region *b* scattering comes from the microporous structure. The slope to the right of the shoulder is identified with surface scattering from the high internal surface area of the carbon (László et al. 2004, László and Geissler). The broad peaks labelled *c, d* and *e* located in the conventional wide angle X-ray scattering (WAXS) range, enlarged in the inset of Fig 2, are residues of the main diffraction peaks of graphite (Bernal), in which the long range order is replaced by short range liquid-like order. The absence of sharp diffraction peaks in this region shows that the sample is free from microcrystalline graphite or impurities.

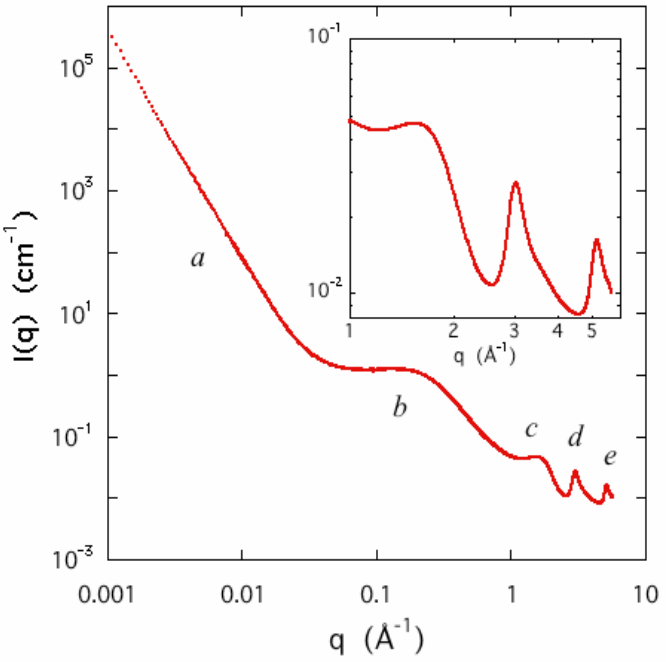

Figure 1. SAXS spectrum of dry sample APETA with regions *a* - *e* described in the text. Inset shows WAXS region (zones *c* – *e*) where the absence of Bragg reflections indicates that the carbon is amorphous.

The SAXS results in all cases exhibit regions where the scattering intensity from the water-containing specimens significantly exceeds that of the dry sample, i.e., cluster formation occurs, even in the most highly oxidized carbon, APETB. This situation is illustrated in Figure 2 for APETA by the strongly negative values of the density function $p(q)$ at q<0.1 Å^{-1}. To establish a quantitative comparison between the macroscopic isotherms and the SAXS results, perturbations from such liquid-vapour interfaces must be minimized. We therefore restrict attention to the higher q-range of the spectrum, where the ratio of the liquid/vapour interfacial area to that of the solid/liquid or solid/vapour is small. In the Porod approach, the intensity scattered by the pore surfaces at the high-q end of the SAXS spectrum (final slope method) is proportional to the surface area of the sample S/V (Porod). Thus

$$I(q) = Kq^{-4} + b, \tag{7}$$

where $K=2\pi[\rho_C - p(q)\rho_S]^2 S/V$ and b is a constant that simulates the signal from the atomic disorder in the sample. The data from the region of scattering from pores should therefore display straight line behaviour when plotted in the form

$$I(q)\, q^4 = K + b\, q^4, \tag{8}$$

Figure 3 shows the results from the Porod scattering region in APETB for different RH, from which the values of the intercept K are obtained. The corresponding expression for $p(q)$ in this high-q range is obtained by comparison with Eq (6). Thus

$$p(\infty) = \rho_C\,[1 - (K/K_{dry})^{1/2}]\,/\rho_S \tag{9}$$

where K_{dry} is the "final slope" of the dry reference sample and K that of the sample exposed to water vapour. (For convenience the symbol ∞ is used here to designate the region 0.6<q<1 Å^{-1} where the values of K are determined.)

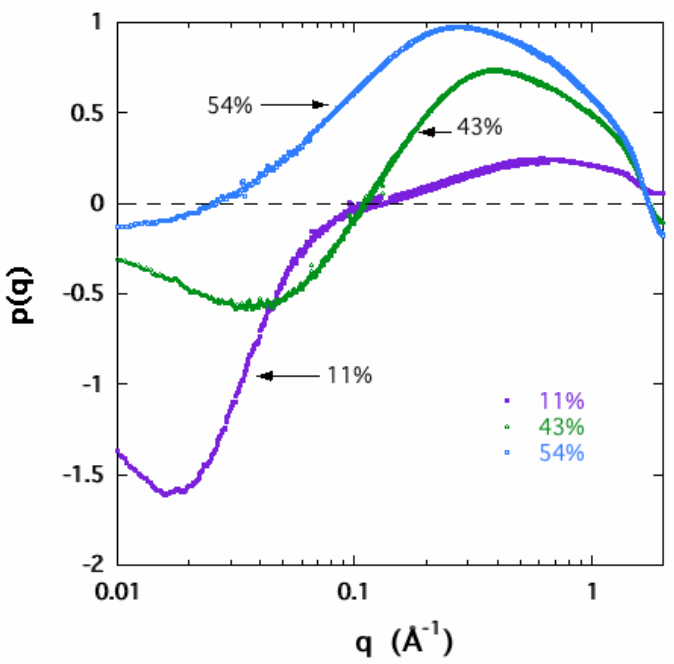

Figure 2. Density function $p(q)$ of water in APETA for three values of RH, 11%, 43% and 56%, calculated from Eq. (6). For clarity, only 20% of the data are shown.

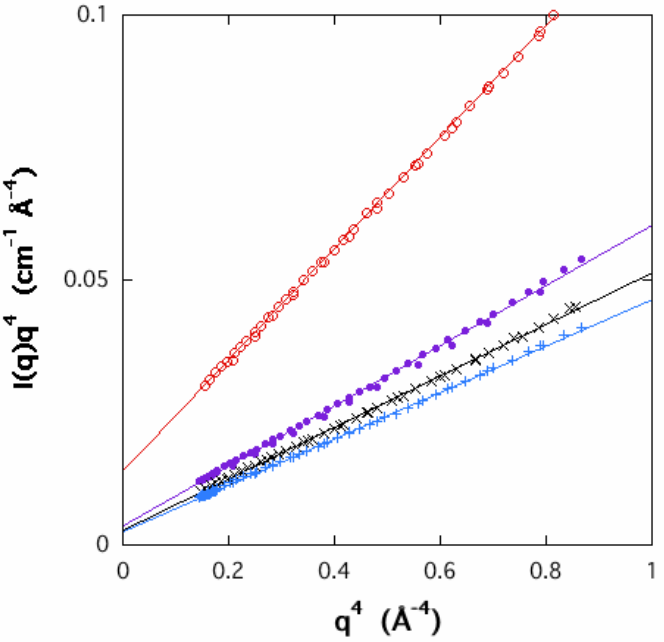

Figure 3. Plots of scattering intensity $I(q)q^4$ versus q^4 from sample APETB for RH= 0% (open circles), 11% (filled symbols), 23% (×) and 33% (+). The intercepts yield the value of K.

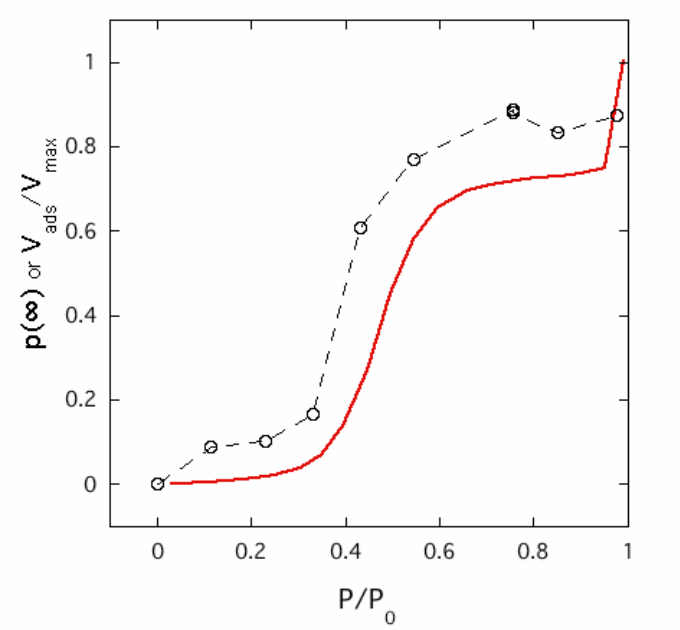

Figure 4. Normalized H_2O adsorption isotherms for APETA with respect to the maximum adsorption, compared with $p(q)$ (open circles) from the final slope region ($0.6<q<1$ Å^{-1}). Note that even at the highest P/P_0 the smallest micropores (8.4 Å $\leq w\ (=2\pi/q) \leq$ 10 Å) are incompletely filled.

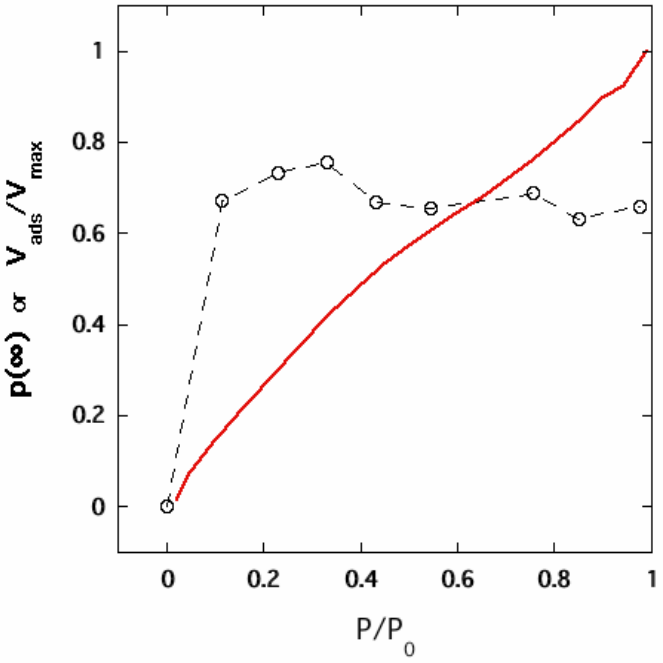

Figure 5. Normalized H_2O adsorption isotherms for APETB, compared with $p(q)$ (open circles) calculated from the final slope region ($0.6<q<1$ Å^{-1}). For $P/P_0 \geq 0.11$ the density of the adsorbed water in the micropores is essentially constant. Dashed lines are guides for the eye.

Figures 4 and 5 compare the SAXS measurements of adsorption of water vapour in the microporous region and the adsorption isotherms, normalized with respect to the maximum adsorption, expressed as V_{ads}/V_{max}. In APETA (Figure 4) the same trend is observed between the two different measurements, with, however an initial step of $p(\infty)\approx 0.1$ that is not replicated in the isotherm. The difference in these responses is due to the different conditions of sample preparation, notably the exposure time to the H_2O vapour and its concentration. The adsorption

measurements on the Hydrosorb instrument were made with vapour generated at 100 °C in a few hours, while the SAXS samples were exposed to water vapour of various RH at 20 °C for two months. For APETB, the difference between the two observations is even more marked. The equilibrium value of $p(\infty)$ is independent of RH for RH>0 over the whole range explored, while the adsorption isotherm reveals a much gradual behaviour. Once again, these results indicate that slow rearrangements of the adsorbed H_2O vapour occur within the carbon, possibly combined with ageing of the surface functional groups. It is also remarkable that the maximum density of water is greater in APETA than in APETB. This finding suggests that in the latter case access to the pores may be blocked by water molecules adsorbed on functional groups located at the entrance of the pores, thus hindering the passage of further adsorbates. The shape of all the SAXS curves reflects a complex distribution that is at least bimodal. These results illustrate the strong effect of surface chemistry on the water adsorption of carbons.

The adsorption behaviour of the Norit R1 sample is similar to that of APETA. The time dependence of the SAXS spectra in the high-q range shows that the pore filling process by water vapour evolves over several weeks.

Conclusions

Activated carbons investigated by small angle X-ray scattering displayed significant differences in the way water vapour is adsorbed that depend on their prior surface-treatment. Lightly oxidized samples (APETA) display significant cluster formation in the macroporous region, while in the heavily oxidized sample (APETB) cluster formation is more limited. In the latter, pore filling by water is constant over the whole range of RH explored (0-98%) and does not exceed about 70%. Micropore filling in the more lightly oxidized sample, however, tends to mimic the adsorption isotherm. At high relative pressure, it is greater than in APETB, an effect that is attributed to steric hindrance by water clusters around functional groups at the entrance to the pores. Differences between the adsorption isotherms and the SAXS results are attributed to the effects of rearrangement and/or ageing in the sample. Direct measurements of the time dependence of the micropore filling in the Norit R1 sample shows that equilibration times with water vapour are of the order of several weeks.

Acknowledgements

The European Synchrotron Radiation Facility is gratefully acknowledged for access to the small angle beamline BM2. We express our warm thanks to G. Bosznai and C. Rochas for their invaluable assistance. This research was supported by the EU - Hungarian Government joint fund (GVOP - 3.2.2 - 2004 - 07 - 0006/3.0).

References

Antxustegi M. M., P.J. Hall and J.M. Calo 1998 Development of Porosity in Pittsburgh No. 8 Coal Char As Investigated by Contrast-Matching Small-Angle Neutron Scattering and Gas Adsorption Techniques. *Energy & Fuels* 12,542–546.

Bernal, J. D. 1924. The Structure of Graphite. *Proceedings of the Royal Society of London. Series A, Containing Papers of a Mathematical and Physical Character, Vol. 106, No. 740*, pp. 749-773.

Bóta, A., K. László, L.G. Nagy and T.A. Copitzky 1997. Comparative study of active carbons from different precursors. *Langmuir* 13, 6502-6509.

Hoinkis, E. 2004. Small-angle Scattering Studies of Adsorption and of Capillary Condensation in Porous Solids. *Part. Part. Syst. Charact*. 21, 80 – 100.

László K. and E. Geissler 2006. Surface Chemistry and Contrast-Modified SAXS in Polymer-Based Activated Carbons. *Carbon* 44, 2437-2444.

László K., K. Marthi , C. Rochas, F. Ehrburger-Dolle, F. Livet and E. Geissler 2004. Morphological Investigation of Chemically Treated PET-based Activated Carbons. *Langmuir* 20, 1321-1328.

László K., O. Czakkel, K. Josepovits, C. Rochas and E. Geissler 2005. Influence of surface chemistry on the SAXS response of polymer-based activated carbons. *Langmuir* 21, 8443-8451.

Lozano-Castelló D., D. Cazorla-Amorós, A. Linares-Solano, P.J. Hall, D. Gascon and C. Galan 2001. In situ small angle neutron scattering study of CD_4 adsorption under pressure in activated carbons. *Carbon*, 39, 1343-1354.

Mitropoulos A.C., J.M. Haynes, R.M. Richardson and N.K. Kanellopoulos 1995. Characterization of porous glass by adsorption of dibromomethane in conjunction with small-angle X-ray scattering. *Physical Review B* 52, 10035-10042.

Porod, G. 1983. In *Small Angle X-ray Scattering*. O. Kratky, O. Glatter (Ed.), Academic Press, New York.

Ramsay J.D.F. 1993. Applications of neutron scattering in investigations of adsorption processes in porous materials. *Pure & Appl. Chem*. 65(10), 2169-2174.